



# Karbala International Journal of Modern Science

Manuscript 3406

**Computational approach: 3D-QSAR, molecular docking, molecular dynamics simulation investigations, drug- like-ness, and DFT score evaluation of a potential novel and retrosynthesis of some TR-H derivatives as Streptococcus pneumoniae drug.**

BELAIDI Mustapha

TCHOUAR Nouredine

DJELILATE Mohammed

Saleh Bufarwa

Dalal K. Thbayh

Follow this and additional works at: <https://kijoms.uokerbala.edu.iq/home>



Part of the [Biology Commons](#), [Chemistry Commons](#), [Computer Sciences Commons](#), and the [Physics Commons](#)



University of  
**Kerbala**

---

## Computational approach: 3D-QSAR, molecular docking, molecular dynamics simulation investigations, drug- like-ness, and DFT score evaluation of a potential novel and retrosynthesis of some TR-H derivatives as *Streptococcus pneumoniae* drug.

### Abstract

*Streptococcus pneumoniae* is the main source of hospital-acquired *pneumonia* and *meningococcal pneumonia* in children, adults, and the elderly, especially the *immunocompromised*. Recently, it has attracted the attention of many research studies around the world as a potential target for remediation. TR-H are considered SP antibacterial agents, as they can inhibit. To describe their mode of action and to identify new antibacterial drugs against *Streptococcus pneumoniae* exhibiting the TR-H scaffold, the present work included 3D-QSAR, *in-silico* pharmacokinetic evaluation and molecular simulation modelling of TR-H. Using an atom-based method for quantitative structure-activity relationship (QSAR) study, a comprehensive 3D-QSAR model was developed using advantageous statistical parameters; the data exhibits a strong correlation, reflected in an  $R^2$  value of 0.9826. The cross-validation score is 0.9667, accompanied by an F-value of 72.7. The model's predictive capabilities were validated through a series of external evaluations and tests. Furthermore, the active compounds underwent a thorough evaluation of their ADMET characteristics and drug similarities, yielding favourable outcomes. In addition, molecular docking studies demonstrated the optimal interactions between these inhibitors and their target receptor. Furthermore, the stability of compounds 5u3 and 5u is confirmed by molecular dynamics simulation for 100 ns. This research contributes to the design of new antibacterial compounds and highlights the importance of computational methods in accelerating the development of therapeutic agents, particularly in controlling infectious diseases

### Keywords

TR-H; DFT; MD simulations; molecular docking; 3D-QSAR; ADME prediction.

### Creative Commons License



This work is licensed under a [Creative Commons Attribution-Noncommercial-No Derivative Works 4.0 License](https://creativecommons.org/licenses/by-nc-nd/4.0/).

## RESEARCH PAPER

# Computational Approach: 3D-QSAR, Molecular Docking, Molecular Dynamics Simulation Investigations, Drug-likeness, and DFT Score Evaluation of a Potential Novel and Retrosynthesis of Some TR-H Derivatives as *Streptococcus pneumoniae* Drug

Belaidi Mustapha<sup>a,b</sup>, Tchouar Nouredine<sup>a</sup>, Djelilate Mohammed<sup>c</sup>,  
Saleh Bufarwa<sup>d</sup>, Dalal K. Thbayh<sup>e,f,g,\*</sup>

<sup>a</sup> Physical Chemistry Department, Chemistry Faculty, University of Sciences and Technologies of Oran (USTO), Laboratory of Process Engineering and Environment (LIPE), BP 1503, Oran, 31000, Algeria

<sup>b</sup> Chemistry Department, Science of Matter, Faculty of Sciences and Technologies, Ahmed ZABANA University, 48000, Relizane, Algeria

<sup>c</sup> Department of Biology, Faculty of Sciences, University of Oran1, Laboratory of Applied Microbiology, BP 16, Es-senia, 31100, Oran, Algeria

<sup>d</sup> Chemistry Department, Omar Al-Mukhtar University, El-Beida, Libya

<sup>e</sup> Institute of Chemistry, University of Miskolc, Miskolc-Egyetemváros, 3515, Hungary

<sup>f</sup> Polymer Research Center, University of Basrah, Basrah, Iraq

<sup>g</sup> Higher Education and Industrial Cooperation Centre, University of Miskolc, Miskolc-Egyetemváros, 3515, Hungary

## Abstract

*Streptococcus pneumoniae* is the main source of hospital-acquired pneumonia and meningococcal pneumonia in children, adults, and the elderly, especially the immunocompromised. Recently, it has attracted the attention of many research studies around the world as a potential target for remediation. TR-H are considered SP antibacterial agents, as they can inhibit. To describe their mode of action and to identify new antibacterial drugs against *Streptococcus pneumoniae* exhibiting the TR-H scaffold, the present work included 3D-QSAR, *in-silico* pharmacokinetic evaluation and molecular simulation modelling of TR-H. Using an atom-based method for quantitative structure-activity relationship (QSAR) study, a comprehensive 3D-QSAR model was developed using advantageous statistical parameters; the data exhibits a strong correlation, reflected in an  $R^2$  value of 0.9826. The cross-validation score is 0.9667, accompanied by an F-value of 72.7. The model's predictive capabilities were validated through a series of external evaluations and tests. Furthermore, the active compounds underwent a thorough evaluation of their ADMET characteristics and drug similarities, yielding favourable outcomes. In addition, molecular docking studies demonstrated the optimal interactions between these inhibitors and their target receptor. Furthermore, the stability of compounds 5u3 and 5u is confirmed by molecular dynamics simulation for 100 ns. This research contributes to the design of new antibacterial compounds and highlights the importance of computational methods in accelerating the development of therapeutic agents, particularly in controlling infectious diseases.

**Keywords:** TR-H, DFT, MD simulations, Molecular docking, 3D-QSAR, ADME prediction

---

Received 7 December 2024; revised 22 April 2025; accepted 25 April 2025.  
Available online 23 May 2025

\* Corresponding author at: Institute of Chemistry, University of Miskolc, Miskolc-Egyetemváros, 3515, Hungary.  
E-mail address: kemdalal@uni-miskolc.hu (D.K. Thbayh).

<https://doi.org/10.33640/2405-609X.3406>

2405-609X/© 2025 University of Kerbala. This is an open access article under the CC-BY-NC-ND license (<http://creativecommons.org/licenses/by-nc-nd/4.0/>).

## 1. Introduction

The increasing prevalence of antibiotic resistance, particularly in pathogens such as *Streptococcus pneumoniae* (SP), has necessitated the urgent need for novel therapeutic strategies [1,2]. This bacterium remains a significant public health threat, implicated in various serious infections, including pneumonia, septicemia, and meningitis, despite widespread vaccination efforts and antibiotic use [3]. The ability of SP to develop resistance mechanisms against conventional antibiotics underscores the limitations of existing treatments and highlights the need for innovative drug discovery approaches [4]. This dissertation addresses the pressing research problem of identifying and characterizing new molecular entities that can effectively target antibiotic-resistant SP [5]. To this end, the integration of advanced computational methodologies—specifically, 3D-QSAR modelling [6], molecular docking [7], molecular dynamics simulations [8], ADMET analysis [9], drug-likeness assessments, and density functional theory (DFT) evaluations [10], will be employed to optimize the design and evaluation of a novel 1,2,3-triazole-hybrid drug (TR-H) [11–13]. This multifaceted exploration aims to identify crucial molecular interactions and mechanisms underpinning the efficacy of the hybrid drug against SP, thereby contributing valuable insights into the field of antimicrobial drug design. The aim of this research is to evaluate the potential efficacy and safety of a novel TR-H drug targeting SP through integrated 3D-QSAR, molecular docking, molecular dynamics simulations, ADMET profiling, drug-likeness assessments, and DFT score evaluations, addressing the key issue of optimizing molecular interactions and pharmacological properties to combat antibiotic resistance; to effectively resolve this problem, comprehensive quantitative data on molecular interactions, conformational stability, and biochemical properties of the compound will be necessary. This research project has the potential to create the next generation of antibacterial medications, addressing the urgent need for creative alternatives to treat SP resistance to beta-lactam antibiotics.

## 2. Materials and methods

### 2.1. Data set-up and structural alignment

A series of 24 TR-H were selected from literature and analyzed using an automated ligand alignment procedure [14]. Compound 5u was used as the template. Charge neutralization, stereoisomer

generation, and ionization state adjustments were performed using Lig-prep software. All 24 structures were aligned using a sampling procedure with 1000 conformers at pH  $7.2 \pm 0.2$  using OPLS-2005 (force field) [15].

### 2.2. 3D-QSAR models

The model 3D-QSAR constructs by incorporating its biological activity values. It was based on default parameters and 100 conformers were produced, with a limit of 10 conformers per rotating bond. The configurations of the molecules were modified, preserving only one alignment for each ligand. Random division was used to assess the model's resilience. The allocation of test sets and training sets was done using an automated random method, with a training set and test set ratio of 75 %. The test set was chosen accurately, following Galbraith and Tropsha's recommendations [16,17].

### 2.3. Validation of the model

According to Tropsha and She, the average pairwise distance (APD) must be established. Consequently, only predictions for compounds within this defined domain can be considered reliable. The APD can be calculated using two commonly used methods: the extent of the extrapolation method, as described by Tropsha, and the Quantitative Structure-Activity Relationship (QSAR) model. The extent of extrapolation determines the degree of extrapolation by calculating the leverage ( $h_i$ ) for each chemical compound. The QSAR model was subsequently used to measure the activity of each compound [16].

$$h_i = x_i^T (X^T X)^{-1} x_i^T \quad (1)$$

$$i(i=1, 2, 3, \dots, n), X(n \times k^{-1})$$

The Equation (1) uses a row vector  $x_i$  to represent the  $k$  query compound model parameters, with  $X$  representing a matrix of dimensions  $(n, x, k)$ . High values of 3000 per unit of normal force indicate unreliable outcomes. The forecast becomes less accurate when the average pairwise distance between a test set and its closest neighbour in the training set is above a certain limit.

$$ADP = \langle d \rangle + Z\sigma \quad (2)$$

The process involves calculating the mean Euclidean distance for each compound combination in the training set, generating a compilation of distances below the mean value, computing the mean

and standard deviation, setting a threshold of 0.5, and incorporating Enola's domain as a similarity node. The Y-randomization technique enhances the reliability of 3D-QSAR models by enabling the creation of tailored models for specific methodologies and datasets [18].

#### 2.4. Molecular docking and dynamic simulation studies

The experimental crystal receptor PBP2x (from SP) was downloaded from [www.rcsb.org](http://www.rcsb.org) (PDB-Code:1QMF, resolution 2.4 Å) [19]. The UCSF Chimera software version 1.18 was used to minimize and add a hydrogen bond to the receptor compound 5u from the 3D-QSAR model, which is the best since it has a good pIC<sub>50</sub> value for creating novel SP drugs for docking molecular analysis of three new inhibitors (5u1, 5u2, and 5u3) proposed using the precedent model, the CB-Dock2 server [20]. The binding cavity was located within a spherical restriction with a radius of 15 units, centering the protein cavity (X = 22.91, Y = 1.31, and Z = 27.91). The ideal docked structure was determined using the corresponding docking scores, as shown in Table 3. Molecular dynamics simulation (MDS) analysis was performed using the Desmond 2022-2 version for the molecules 5u and 5u3. The simulations were conducted in the canonical ensemble, where the number of atoms, pressure, and temperature were kept constant (NPT). Force fields (OPLS3e) were used for molecular dynamic simulations of compounds, with initial systems created using the TIP3P water model. Neutralizing systems with Na<sup>+</sup>/Cl<sup>−</sup> ions was done using a 100-ps Brownian motion MDS in an NVT ensemble. The equilibrated systems were then subjected to a 100-ps simulation in the NPT ensemble. The RMSD, RMSF, number of protein-ligand interactions, and interaction fractions were calculated in this study [21]. A protein-inhibitor combination stability simulation was carried out to examine the simulation results and identify the most interesting new inhibitor.

#### 2.5. Density Functional Theory (DFT) and Frontier Orbital Calculations

The DFT calculations were performed using the Orca 5.0.4 software package, employing the M06 functional and the 6–311G(d) basis set [22]. This functional and basis set was selected based on an analysis of the molecular structure (bond distance and angle of 5c). (Fig.S1a) ([https://kijoms.uokerbala.edu.iq/cgi/editor.cgi?article=3406&window=additional\\_files&context=home](https://kijoms.uokerbala.edu.iq/cgi/editor.cgi?article=3406&window=additional_files&context=home)) and a comparison

between the experimental data (X-ray) and calculated data (refer to Tab. S1a in the Supporting Information Data) [14]. The newly developed inhibitors (5u1, 5u2, and 5u3) were also studied by using the M06/6–311G(d). The electronic characteristics determined in the investigation for the chosen compounds align with their respective reactivity.

#### 2.6. Drug-likeness/ADMET evaluations

The preliminary assessment of the absorption, distribution, metabolism, excretion, and toxicity (ADMET) properties of possible candidates and their similarities with existing medications is an essential step in the drug development process. Therefore, this evaluation identifies various significant outcomes and is one of the most critical steps. The ADMET effects of oral medications are related to several different pharmacokinetic indices [23]. In this investigation, the Swiss ADME web server and Osiris software were used to calculate physicochemical descriptors and predict the ADME parameters, pharmacokinetic characteristics, drug-likeness features and pharmaceutical chemistry properties for the new 5u1, 5u2, and 5u3 inhibitors [24].

### 3. Results and discussion

#### 3.1. Visualization of 3D-QSAR models

Energy minimization was performed for each conformer studied (Fig. 1). SD: Regression standard deviation; R<sup>2</sup>: Regression factor; F: Ratio of model variance to observed activity variance; P: Variance ratio consistency level; Q<sup>2</sup>: Cross-validated correlation factor in the test set; RMSE: Root mean squared error of test set predictions. This research, which was performed using the atom based method, unearthed vital information regarding the impact of substitution on the observed activity. The 3D-QSAR

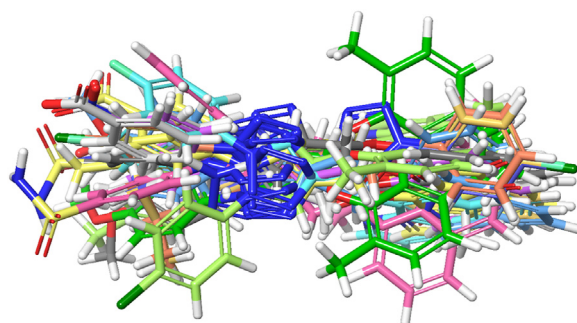


Fig. 1. Twenty-four ligands before alignment.



model was constructed using the least partial squares (PLS) regression analysis technique inside a grid space of 1.0 Å. Seven models were shown to have a gradually increasing level of statistical significance and predictability; the number of PLS factors incorporated into the construction of the model was set at seven (Table 1). The PLS-7 model provided the best fit ( $R^2 = 0.9826$ ,  $Q^2 = 0.9667$ , and  $F = 72.7$ ). This insight becomes much more apparent when one considers the inference of survival inactivity in contrast to the activity of survival.

### 3.2. Validation of the model and its applicable domain

The cross-validation coefficient ( $Q^2 = 0.9667$ ) (Table 1) assessed the accuracy and dependability of the commonly used PLS-7 model (test set) for identifying results. The regression factor for the training set was 0.9826, indicating a solid level of relevance for the PLS-7 model. We observed the stability of the model, which varied between 0.372 and 0.825 on a maximum scale of one. In addition, the  $F$  value is 72.7. Furthermore, the model exhibited a higher confidence level, as evidenced by a  $P$  value of  $3.35E-07$  and a Pearson correlation coefficient of 0.9862. The created model for predicting unknown substances in the test exhibited stability, as shown by an SD (standard deviation) of 0.0604 and the cross-validated correlation factor in the set test (RMSE) of 0.06. The scatter plots in Fig. 1(a) and (b) demonstrate a substantial linear association and a considerable disparity between the ligands' experimental and anticipated activities. An external test set was utilized to assess the effectiveness of the constructed model for further validation. The  $pIC_{50}$  values for substances in the planned and external test series are shown in Table 2 and Fig. 2 compares the experimental activity and predicted activity ( $pIC_{50}$  predicted 7) and the relationship between the anticipated  $pIC_{50}$  predicted and the residual  $pIC_{50}$ .

An external test set was utilized to assess the effectiveness of the constructed model for further validation. The  $pIC_{50}$  values for substances in the

Table 2. Predicted  $pIC_{50}$  for the TR-H compounds <sup>t</sup>: denoted test set.

Compound	R	$pIC_{50}$ Exp. [21]	$pIC_{50}$ pred. 7	Residue $pIC_{50}$
5a <sup>t</sup>	H	2.813	2.81	0.003
5b	F	3.014	2.984	0.03
5c <sup>t</sup>	Cl	3.047	3.033	0.015
5d	NO <sub>2</sub>	2.853	2.849	0.004
5e	COOH	3.749	3.496	-0.564
5f	Me	2.932	2.983	-0.051
5g	OMe	3.749	3.751	-0.002
5h	SO <sub>2</sub> NH <sub>2</sub>	2.829	3.735	-0.906
5i	H	3.063	3.058	0.005
5j <sup>t</sup>	F	2.929	3.232	-0.303
5k	Cl	3.09	3.281	-0.191
5l <sup>t</sup>	NO <sub>2</sub>	3.299	3.096	-0.006
5m	COOH	3.514	3.744	-0.23
5n	Me	3.448	3.231	0.217
5o <sup>t</sup>	OMe	3.306	3.999	-0.693
5p	SO <sub>2</sub> NH <sub>2</sub>	3.534	3.985	-0.95
5q <sup>t</sup>	H	3.416	3.292	0.242
5r	F	2.488	3.466	-0.05
5s	Cl	3.035	3.515	-1.027
5t <sup>t</sup>	NO <sub>2</sub>	3.033	3.33	-0.297
5u	COOH	3.979	3.977	0.002
5v <sup>t</sup>	Me	3.512	3.465	0.047
5w	OMe	3.535	3.534	0.001
5x	SO <sub>2</sub> NH <sub>2</sub>	3.682	4.217	-0.535

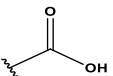
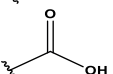
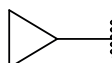
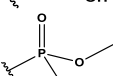
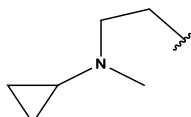
planned and external test series are shown in Table 2 and Fig. 2, which compares the experimental activity and predicted activity ( $pIC_{50}$  predicted 7) and the relationship between the anticipated  $pIC_{50}$  predicted and the residual  $pIC_{50}$ . The structures utilized are based on the 1,2,3-triazole cycle incorporating three natural products (carvacrol, 2-hydroxynaphthoquinone, and 2-hydroxyquinoline).

The model's reliability was confirmed through  $Y$  randomization, with low  $R^2$  and  $Q^2$  values indicating that the positive results are not due to random chance or reliance on the training dataset's structure (Table 1). It is essential to recognize that the training dataset approach has been meticulously followed for each statistical permutation of vector  $Y$  to build the new 3D-QSAR model, to ascertain a link between the empirical and projected  $pIC_{50}$  values of the PLS-7 model (Fig. 3).

Table 1. The statistical details of the models (PLS).

PLS	SD	$R^2$	F	P	Stability	RMSE	$Q^2$	Pearson-R
1	0.1494	0.8231	69.8	$5.03E-07$	0.825	0.13	0.8236	0.9317
2	0.1209	0.8919	57.8	$1.72E-07$	0.669	0.11	0.8574	0.9402
3	0.1097	0.9173	48.1	$2.69E-07$	0.551	0.08	0.9344	0.979
4	0.0784	0.961	74	$2.37E-08$	0.407	0.07	0.9405	0.9855
5	0.0583	0.9803	109.3	$5.39E-09$	0.354	0.06	0.9605	0.9836
6	0.0584	0.982	90.8	$3.89E-08$	0.372	0.06	0.9668	0.9864
7	0.0604	0.9826	72.7	$3.35E-07$	0.372	0.06	0.9667	0.9862

Table 3. The molecular structures of the newly created effective substances and compound 5u.

Cp.	R <sup>1</sup>	R <sup>2</sup>	R <sup>3</sup>	R <sup>4</sup>	R <sup>5</sup>	R <sup>6</sup>	R <sup>7</sup>	Pre-pIC <sub>50</sub>
5u		H	H	H	H	H	H	3.977
5u1			H	H	H	H	H	2.993
5u2		H	H	H	H	H	H	2.997
5u3	H	H	H	H	H	H		3.035

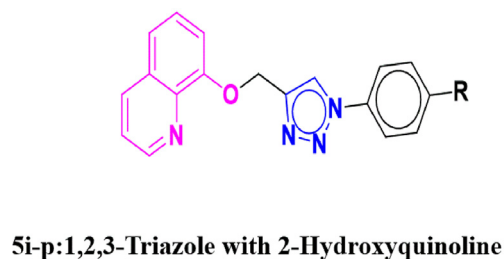
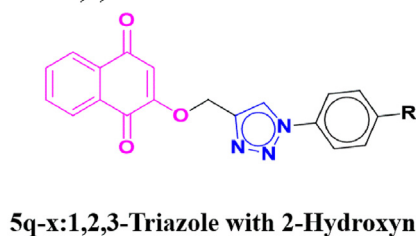
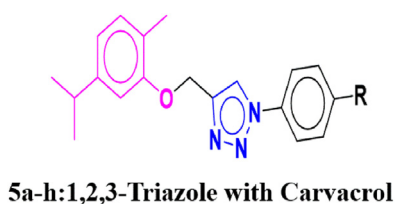
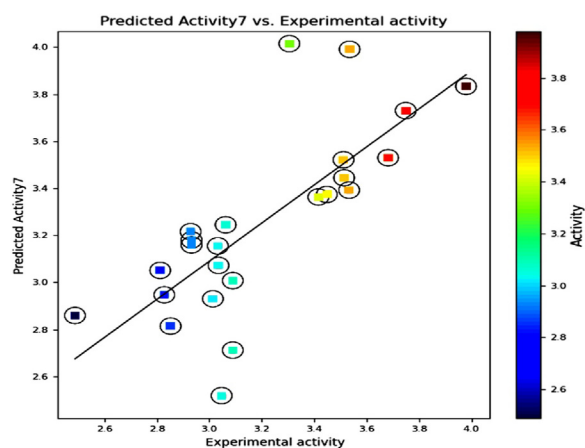


Fig. 2. Chemical structures of the TR-H.

### 3.3. Study of 3D-QSAR contour maps showing favorable and unfavorable conditions

To investigate how the spatial arrangement was felt, a contour analysis was carried out of molecular attributes, such as electrostatics, ionic, hydrophobic, hydrogen bond donor, and hydrogen bond acceptor regions, on the antibacterial efficacy against *SP*. The blue cubes represent the excellent contributions made by each group, while the red cubes denote the negative contributions. Fig. 4(a–e) illustrates the prominent and unfavourable interactions observed when using the 3D-QSAR model for the most and the smallest active compounds. Compound 5u

Fig. 3. Plot scatter plots of exp vs. pred pIC<sub>50</sub> (activity) 7 ( $y = 0.94x + 0.37$ ,  $R^2 = 0.92$ ).

(Fig. 4a) had a greater propensity for hydrogen-bond donation than compound 5x did (as depicted in Fig. 4b). The distinction was observed by allocating the blue color to the most advantageous areas and the red colour to the disadvantageous regions. The mapping of hydrogen bond donors demonstrated that regions with good characteristics were close to the acid group of benzoic acid, which is positioned at the first position of the 1,2,3-triazole (Fig. 4a). This observation implies that these locations substantially influence the compound's action.

The 3D-QSAR model depicted compounds 5w (3.535), 5e (3.749), 5i (3.063), and 5o (3.306) to have favourable and unfavourable hydrophobic interactions, while compound 5u was the most active and lacked an acid group at the correct steric site (Fig. 4b). Hence, the inclusion of 2-hydroxynaphthoquinone, which contains an acid group that donates hydrogen, is crucial for its bacteriostatic effect. Additionally, compounds with 8-hydroxyquinoline moieties have lower activity than those with 2-

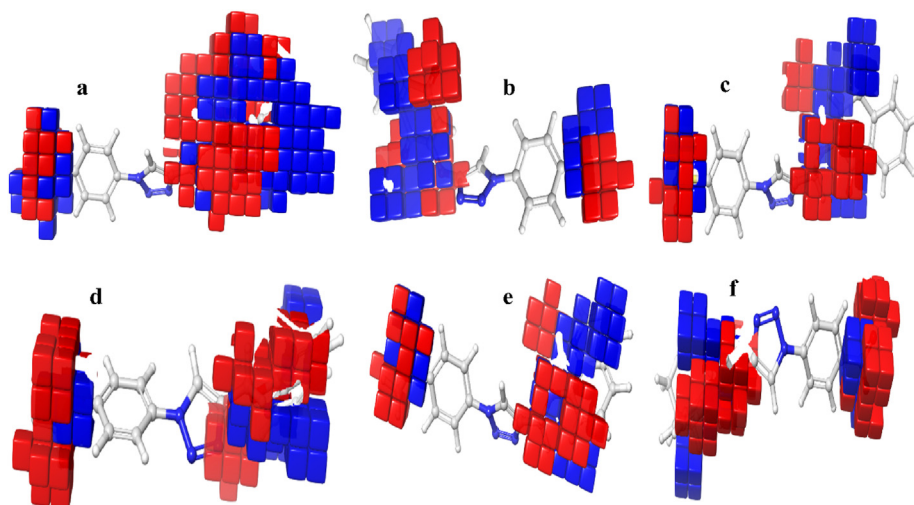


Fig. 4. 3D-QSAR model with favorable and unfavorable hydrogen bond donor effects for compounds 5u (a) (3.979) and 5x (b) (3.682).

hydroxynaphthoquinone moieties (5 (q–x)). The significance of the quinoline molecule's action can be inferred by the presence of blue cubes adjacent to the oxygen atom of the 2-hydroxynaphthoquinone ring, which is connected to the fifth and sixth carbon positions.

This contrasts with compound 5w, which lacks the ring mentioned earlier in its backbone structure and exhibits lower activity. In this context, the carvacrol derivative 5 (a–h) showed greater potency than the carvacrol derivative 5e. This suggests that introducing a more hydrophilic substituent to the naphthoquinone compound could enhance its inhibitory effect on *SP*. The apparent impacts of the groups that withdraw electrons from the most active and inactive substances can be examined by examining para-linked naphthoquinone with 1,2,3-triazole.

The previously described site has a significant blue zone, indicating electron-withdrawing group replacement. This discovery aligns with the

observed trend in activity, where the substitution of an electron-withdrawing group such as nitro or acid at the para position of naphthoquinone and carvacrol linked to 1,2,3-triazole in compounds 5u, 5t, 5e and 5d leads to a significant decrease in activity. An increase in hydrogen bond donors slows *S.pneumoniae* inhibition. For instance, molecules 5p and 5h have a lower  $pIC_{50}$  value compared to drug 5u. In addition, the colored maps in (Fig. 4a) indicate the presence of a hydrogen bond acceptor field surrounding the R group. This implies that the presence of a donor substitute (such as S, O, or N) in this region has the potential to facilitate the establishment of a hydrogen bond interaction.

#### 3.4. Design of a new compound *SP* inhibitor

Using the current atom-based QSAR by analyzing the model maps and considering the influence of the various groups in Fig. 5 on the inhibitory action of TR-H replacement derivatives, we have

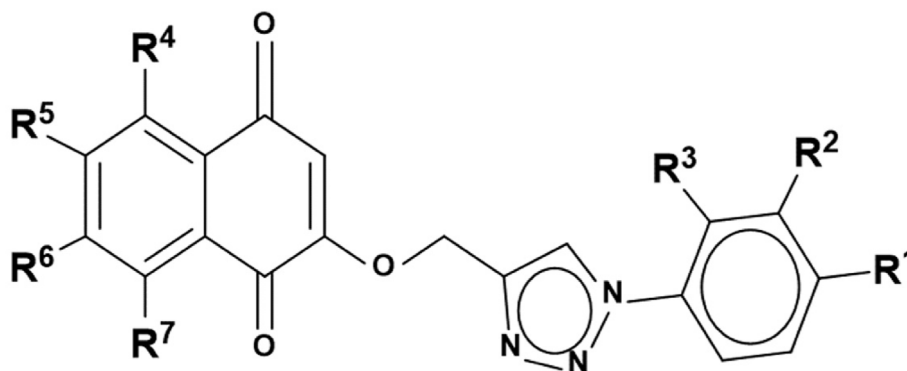


Fig. 5. The chemical structure of TR-H.



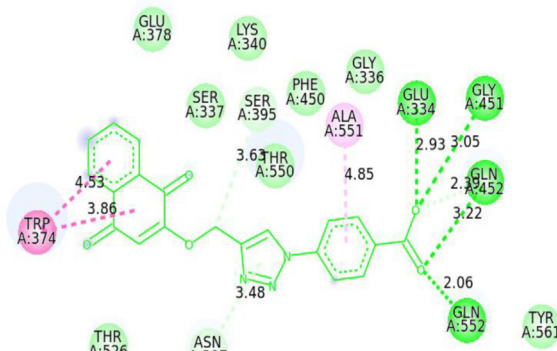
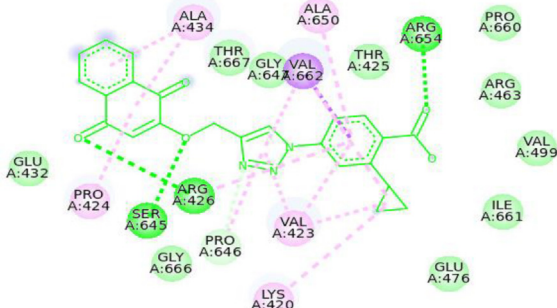
developed novel inhibitors. These compounds were identified based on various contour maps, in which we attempted to substitute the active groups (R1, R2, R3, R4, R5, R6, and R7) with alternative substituents that are both more effective and less electronegative than the substituents found in the 5u molecule. Schrodinger 2022-4 software was subsequently used to assess the biological activity of the compounds. Consequently, we developed three novel compounds, namely 5u1, 5u2, and 5u3, as depicted in Table 3. This table also displays the anticipated  $pIC_{50}$  values of these recently developed highly effective products. The component in the sequence that exhibited the highest level of activity was compared to 5u, 5u1; 5u2 and 5u3 have a high inhibition. In fact, we predict that  $pIC_{50}$  of these compounds are 2.993, 2.997 and 3.035, which are less than the  $pIC_{50}$  of the 5u compound (3.977) (Table 3). In particular, the 5u3 compound should be very effective.

### 3.5. Docking investigation

The RMSD value of 0.594 Å and the superposed of both the docked and the redocked ligands provide

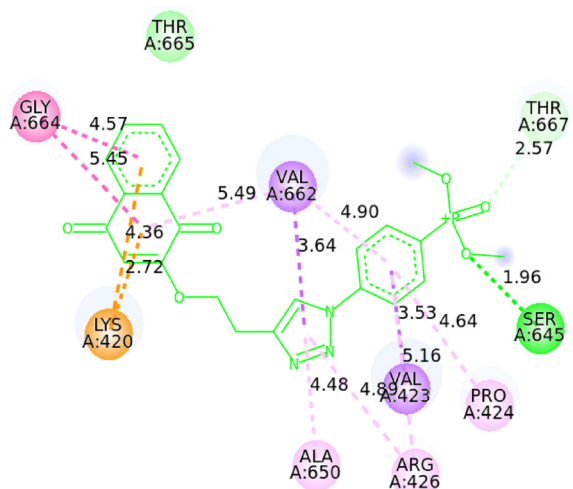
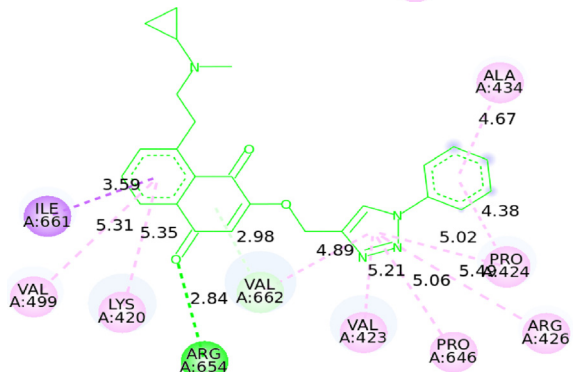
evidence of the accuracy and precision of the docking method (Fig.SI b ([https://kijoms.uokerbala.edu.iq/cgi/editor.cgi?article=3406&window=additional\\_files&context=home](https://kijoms.uokerbala.edu.iq/cgi/editor.cgi?article=3406&window=additional_files&context=home))). The molecular docking research yielded four complexes, specifically emphasizing the 5u1-1QMF, 5u2-1QMF, and 5u3-1QMF complexes because of their elevated binding scores (−10.6, −10.6, and −10.3 kcal/mol) as shown in (Table 4). The specific interactions between the complexes and the important receptor residues are described in (Table 5). Within the reference drug-1QMF complex, various interactions were observed. These included conventional hydrogen bonds with SER395, GLN452, GLN552; and GLN552 carbon-hydrogen bonds and Pi-sigma bonds with ASN397 and TRP374. Typical hydrogen bonds were used to form interactions with PRO646, ARG426, ARG654; and ARG654 in the 5u1-1QMF complex. The distances varied from 2.8 Å to 4.5 Å. Compound 5u2 was found to form three conventional hydrogen bonds with the ARG654, ARG426, SER645, LYS420, LYS420, and VAL662 at distances of 3.16, 3.90, 3.58, 3.22, and 2.84 Å, respectively, as predicted. In addition, two Pi-sigma bonds were formed with residues LYS420 and VAL662. The compound 5u3-1QMF

Table 4. 2D representation of the obtained complexes and corresponding interactions and docking scores (kcal/mol).

Complex	Visualization-2D	Docking score
5u-1QMF (Ref)		−10.7
5u1-1QMF		−10.6

(continued on next page)

Table 4. (continued)

Complex	Visualization-2D	Docking score
5u2-1QMF		−10.6
5u3-1QMF		−10.3
<b>Interactions</b> <div style="display: flex; justify-content: space-between;"> <div> <div style="display: flex; align-items: center;"> <div style="width: 10px; height: 10px; background-color: #90EE90; border: 1px solid black; margin-right: 5px;"></div> van der Waals </div> <div style="display: flex; align-items: center;"> <div style="width: 10px; height: 10px; background-color: #00FF00; border: 1px solid black; margin-right: 5px;"></div> Conventional Hydrogen Bond </div> <div style="display: flex; align-items: center;"> <div style="width: 10px; height: 10px; background-color: #90EE90; border: 1px solid black; margin-right: 5px;"></div> Carbon Hydrogen Bond </div> </div> <div style="display: flex; justify-content: space-between;"> <div> <div style="display: flex; align-items: center;"> <div style="width: 10px; height: 10px; background-color: #90EE90; border: 1px solid black; margin-right: 5px;"></div> Pi-Donor Hydrogen Bond </div> <div style="display: flex; align-items: center;"> <div style="width: 10px; height: 10px; background-color: #FF00FF; border: 1px solid black; margin-right: 5px;"></div> Pi-Pi Stacked </div> <div style="display: flex; align-items: center;"> <div style="width: 10px; height: 10px; background-color: #FF00FF; border: 1px solid black; margin-right: 5px;"></div> Pi-Alkyl </div> </div> </div></div>		

exhibited 5 conventional hydrogen bonds and 3 alkyl bonds with the VAL662, ASN735, ARG654, ILE661; and VAL662 residues. The lengths between these bonds were measured to be 2.42 Å, 2.32 Å, 2.48 Å; and 3.92 Å. The residues that were found in all the complexes obtained were consistent with those observed in the reference drug complex.

### 3.6. ADMET analysis

The findings of the POM analysis provide a thorough evaluation of the recently predicted compounds (5u1, 5u2, and 5u3), emphasizing their significant physicochemical characteristics and potential hazards that are critical for the progress of the development of pharmaceuticals (Table 6). Compound 5u3 demonstrated excellent potential as a candidate agent, exhibiting a favorable profile and no mutagenic, tumorigenic, irritating, or reproductive

hazards. The mild pharmacokinetics, along with a favourable drug score, highlight its potential fit for further research. Compound 5u3 was found to have favourable physicochemical qualities of the medication, including a moderate level of lipophilicity ( $\text{LogP} = 2.24$ ), high solubility ( $\text{LogS} = -4.36$ ), and a molecular weight of 428 g/mol. Compound 5u3 has potential therapeutic applications, but compounds 5u1 and 5u2 pose risks of mutations and tumours, raising safety concerns. Their pharmacokinetics and solubility need careful evaluation. These findings aid in improving compound design and selecting promising candidates for pre-clinical and clinical trials.

### 3.7. Molecular dynamics simulations

#### 3.7.1. Protein-ligand RMSD

The study examined protein 1QMF and a reference structure, as well as protein 1QMF in

Table 5. The interactions between the docked TR-H and the receptor.

Complex	Residues	Interaction Type	Distance (Å)
5u (Ref)-1QMF	SER395	H-Donor	3.63
	GLN452	H-Acceptor	3.22
	GLN552	H-Acceptor	3.01
	GLN552	H-Acceptor	3.38
	ASN397	pi-H	3.48
	TRP374	pi-pi	3.84
5u1-1QMF	TRP374	pi-pi	3.88
	PRO646	H-acceptor	3.47
	ARG426	H-acceptor	3.00
	ARG654	H-acceptor	3.23
5u2-1QMF	ARG654	H-acceptor	3.08
	ARG654	H-acceptor	3.40
	ARG426	H-acceptor	3.60
	SER645	H-acceptor	2.88
	LYS420	pi-cation	4.36
	LYS420	pi-cation	3.61
5u3-1QMF	VAL662	pi-H	3.64
	VAL662	H-donnor	3.13
	VAL662	H-donnor	3.90
	ASN735	H-donnor	3.58
	ARG654	H-acceptor	3.22
	ARG654	H-acceptor	2.84
	ILE661	Pi-H	4.40
	VAL662	Pi-H	3.98
	VAL662	Pi-H	4.33

Table 6. POM evaluation was subsequently conducted on the recently designed compounds 5u1, 5u2, and 5u3.

Molecules	5u1	5u2	5u3
Mutagenic	MR	MR	NR
Tumorigenic	NR	NR	NR
Irritant	NR	HR	NR
Reproductive effect	NR	HR	NR
Clogp	2.25	1.22	2.24
Solubility	-4.94	-3.59	-4.36
Mol-weight	415	453	428
Tpsa	11.3	119.4	77.32
Druglikeness	-7.22	-33.12	2.27
Drug-score	0.26	0.11	0.65

Risk-Indication: Medium risk (MR), High risk (HR), and No risk (NR).

combination with compound 5u3, over a 100 ns simulation period. The RMSD plots showed high alignment between the two graphs, indicating protein structures-maintained stability throughout the simulation and minimal variation from their original conformations. The protein's structure remained intact during molecular dynamics simulation while bound to the compounds.

Ligand RMSD analysis indicated that both the reference 5u drug and compound 5u3 were consistently stable throughout the MD simulation. The control medication maintained an RMSD value < 2.4 Å, indicating a consistent and stable binding conformation with the protein target. Compound 5u3 exhibited robust early stability, with

an RMSD value of 1.5 Å for 60 ns, indicating a strong and consistent interaction with the protein target. Despite a minor increase in the RMSD value to 2.6 Å after 60 ns, it remained within a satisfactory range and decreased to 1.8 Å until the end, indicating stable maintenance of ligand-protein interaction. Robustness and the potential of compound 5u3 as a ligand alternative that warrants further investigation in the pursuit of pharmaceutical advancement (Fig. 6).

### 3.7.2. RMSF

Fig. 7 shows the root-mean-square-fluctuation (RMSF) graph, which shows how flexible and stable different parts of the protein-ligand complex are. Throughout our investigation, we observed limited differences in both complexes, with the interacting residues exhibiting RMSF values that remained between 2–4 Å. Clearly state which residues remain stable and which exhibit flexibility. This observation implies that the positions of these residues remained

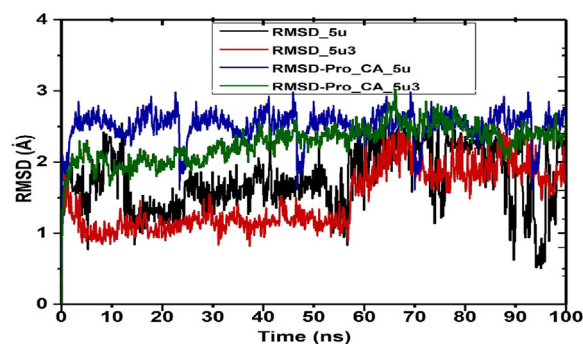


Fig. 6. Plot of the RMSD for both the 1QMF-5u, and 1QMF-5u3 complexes.

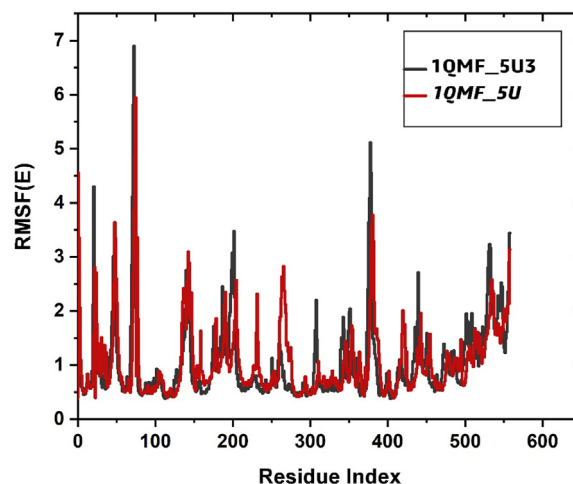


Fig. 7. The RMSF plots for the investigated complexes over the course of the 100 ns simulations.

constant during the simulation, which signifies that their interactions with the ligand were strong and consistent. The low values of RMSF suggest that these residues are engaged in stable binding interactions, hence increasing the overall stability of the protein-ligand. This information further supports the potential of the ligand as a very attractive candidate for therapeutic development by demonstrating the robust and consistent nature of the interactions between the protein and the ligand. Histogram depicting the interaction between a protein and a ligand. The interaction histogram offers useful insights into the nature and occurrence of interactions between the ligand and the crucial residues in the protein binding site (Fig. 7). During our comprehensive examination of all the complexes, we successfully identified the crucial residues that participate in ionic hydrogen bonding and water bridging. The residues were shown to interact with the ligand during the simulation, corroborating the findings of the docking experiments. Ionic hydrogen bonds and water bridges play crucial roles in anchoring ligands within protein binding pockets, enabling robust and precise binding interactions. The consistent occurrence of these interactions emphasizes the significance of these residues in facilitating ligand-protein interactions and enhancing the overall stability of the protein-ligand complex.

### 3.7.3. Protein-ligand interaction histogram

A histogram of interactions is helpful for analyzing nature and the occurrence of interactions between a ligand and crucial residues inside a protein binding region (Fig. SIc ([https://kijoms.uokerbala.edu.iq/cgi/editor.cgi?article=3406&window=additional\\_files&context=home](https://kijoms.uokerbala.edu.iq/cgi/editor.cgi?article=3406&window=additional_files&context=home))).

Through our investigation of both complexes, we identified essential residues that play a role in the creation of ionic hydrogen bonds and water bridges. Throughout the simulation, the residues were shown to interact consistently with the ligand, supporting the findings of the docking experiments. Hydrogen links and water bridges between ions play crucial roles in anchoring ligands within protein binding pockets, enabling robust and precise binding pockets. The fact that these interactions are consistent highlights the importance of these residues in ligand-protein interactions and improves the overall stability of the protein-ligand combination.

### 3.8. Density Functional Theory (DFT) study

The calculation of various quantum chemical properties has relied on the utilization of values pertaining to the energy of the lowest unoccupied

Table 7. The quantum chemical properties of ligands 5u and 5u3 were determined with DFT: M06/6-311G(d).

Quantum chemical parameters of new inhibitor	5u	5u3
$E_{\text{HOMO}}$ (eV)	−7.4614	−6.0669
$E_{\text{LUMO}}$ (eV)	−3.0654	−3.0919
$\Delta E_{\text{GAP}}$ (eV)	4.396	2.975
$\mu$ (Debye)	2.6195	4.5794
$\eta$ (eV)	2.198	1.4875
$\sigma$	0.455	0.6772
$\chi$ (eV)	5.2634	4.5794
$\omega$	6.3019	7.0493

molecular orbital ( $E_{\text{LUMO}}$ ) and the highest occupied molecular orbital ( $E_{\text{HOMO}}$ ), as well as the energy gap ( $\Delta E_{\text{GAP}}$ ), dipole moments ( $\mu$ ), hardness ( $\eta$ ), local softness ( $\sigma$ ), electronegativity ( $\chi$ ) and electrophilicity ( $\omega$ ). The formulas cited in (reference) [25] were used to calculate the parameters mentioned earlier (Table 7).

Quantum chemical calculations help figure out how reactive a molecule is by looking at its hardness ( $\eta$ ), local softness ( $\sigma$ ), electronegativity ( $\chi$ ), and electrophilicity ( $\omega$ ). These parameters are crucial in assessing a molecule's stability and chemical reactivity. Hardness quantifies a molecule's ability to withstand the polarization or deformation of its electron clouds, while local softness indicates a lower energy gap. Electronegativity values show that 5u3 has the highest electronegativity, indicating the lowest electron-donating ability. Electrophilicity characteristics are quantified by a molecule's capacity to accept electrons, with high  $\omega$  values indicating favourable electrophilic nature and low  $\omega$  values indicating good nucleophilic character. Organic compounds can be divided into three groups based on electrophilicity: marginal electrophiles (less than 0.8 eV), moderate electrophiles

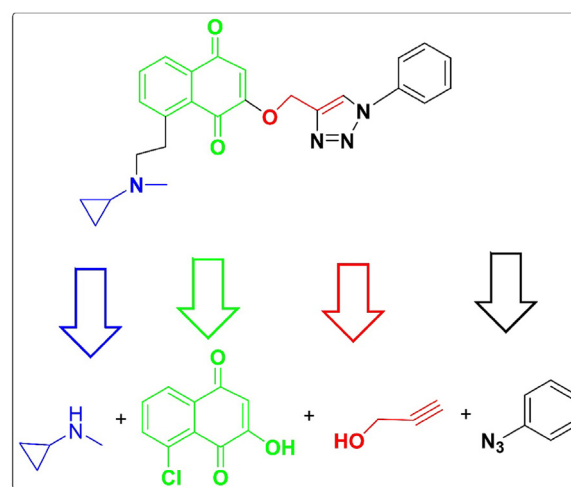


Fig. 8. Retrosynthesis scheme of the studied novel inhibitor (5u3) of *S. pneumoniae*.



(between 0.8 and 1.5 eV), and strong electrophiles (greater than 1.5 eV). The study of compounds reveals moderate electrophilic characteristics, with  $\omega$  values exceeding 1.5 eV, but significant electrophilic character. Overall, these quantum parameters are essential in evaluating a molecule's stability and chemical reactivity. Finally, the retrosynthesis of the newly developed inhibitor is also presented, which will be used in the subsequent synthesis of 5u3 (Fig. 8).

#### 4. Conclusions

An accurate and robust 3D-QSAR model has been developed with outstanding predictive capability when assessing the inhibitory efficacy of TR-H compounds against SP bacteria. Internal and external evaluations have thoroughly confirmed the statistical robustness and predictive ability of the model. The model was applied to predict new compounds with antibacterial activity. In addition, comprehensive silico analysis, including molecular docking, pharmacokinetic/ADMET evaluation, and drug similarity assessment, highlighted promising features of two compounds (5u3 and reference 5u). The molecular dynamic simulation study confirmed the stability of compound 5u3 during a timeframe of 100 ns; the RMSD of both ref 5u and 5u3 demonstrated a clearly small fluctuation, indicating that the two ligands were stable and had high binding affinity to the target 1QMF. To guarantee the accuracy of the computational predictions and accelerate progress in the field of antibacterial therapeutics, the synthesis of the most promising compound (5u3) has been proposed to test it via vitro studies.

#### Consent to participate

Not applicable.

#### Compliance with ethical standards

The authors declare that they have no conflict of interest.

#### Authors' contributions

All authors contributed to the study conception and design. Material preparation and data collection were performed by Mustapha Belaidi, Mohammed Djelilate, and Saleh Bufarwa. Data analysis was performed by Mustapha Belaidi, Noureddine Tchouar, and Dalal K. Thbayh. The final draft of the manuscript was written by Mustapha Belaidi and all authors commented on the manuscript. All authors read and approved of the final manuscript.

#### Data availability

All data generated or analyzed during this study are included in the article and supplementary materials.

#### Consent for publication

Not applicable.

#### Funding

This research is supported by the European Union and the Hungarian State, co-financed by the European Regional Development Fund in the framework of the GINOP-2.3.4-15-2016-00004 project, which aimed to promote the cooperation between the higher education and the industry. Further support was provided by the National Research, Development and Innovation Fund within the TKP2021-NVA-14 project.

#### Conflicts of interest

The authors declare that they have no conflict of interest.

#### Acknowledgements

The authors sincerely acknowledge the *DGRSDT* and the Ministry of Higher Education and Scientific Research of Algeria.

#### References

- [1] L. McGee, M.W. Pletz, J.P. Fobiwe, K.P. Klugman, Antibiotic resistance of pneumococci, in: *Streptococcus Pneumoniae*, Elsevier, 2015, pp. 21–40, <https://doi.org/10.1016/B978-0-12-410530-0.00002-8>.
- [2] A.R. Narciso, R. Dookie, P. Nannapaneni, S. Normark, B. Henriques-Normark, *Streptococcus pneumoniae* epidemiology, pathogenesis and control, *Nat Rev Microbiol* 23 (2025) 256–271, <https://doi.org/10.1038/s41579-024-01116-z>.
- [3] J.E. Meisel, J.F. Fisher, M. Chang, S. Mobashery, Allosteric inhibition of bacterial targets: an opportunity for discovery of novel antibacterial classes, in: J.F. Fisher, S. Mobashery, M.J. Miller, eds., *Antibacterials*, Springer International Publishing, Cham, 2017, pp. 119–147, [https://doi.org/10.1007/7355\\_2017\\_21](https://doi.org/10.1007/7355_2017_21).
- [4] F.-F. Chiu, L.-L. Tu, W. Chen, H. Zhou, B.-S. Liu, S.-J. Liu, C.-H. Leng, A broad-spectrum pneumococcal vaccine induces mucosal immunity and protects against lethal *Streptococcus pneumoniae* challenge, *Emerg Microb Infect* 12 (2023) 2272656, <https://doi.org/10.1080/22221751.2023.2272656>.
- [5] H. Nishiya, Case of pneumococcal (PRSP) bronchitis: gram staining as the earliest and useful indicator for evaluating the effectiveness of antimicrobial therapy in outpatient, *Med Res Arch* 11 (2023), <https://doi.org/10.18103/mra.v11i8.4207>.
- [6] M. Shen, C. Béguin, A. Golbraikh, J.P. Stables, H. Kohn, A. Tropsha, Application of Predictive QSAR models to database mining: identification and experimental validation of novel anticonvulsant compounds, *J Med Chem* 47 (2004) 2356–2364, <https://doi.org/10.1021/jm030584q>.



- [7] M. Khedraoui, H. Nour, I. Yamari, O. Abchir, A. Errougui, S. Chtita, Design of a new potent Alzheimer's disease inhibitor based on QSAR, molecular docking and molecular dynamics investigations, *Chem Phys Impact* 7 (2023) 100361, <https://doi.org/10.1016/j.chphi.2023.100361>.
- [8] Y.-K. Zhang, J.-B. Tong, J. Tan, M. Yang, X.-Y. Xing, Y.-R. Zeng, Z. Xue, C.-J. Tan, Study on the anti-HBV activity of matrine alkaloids from *Oxytropis ochrocephala* by MTT, 3d-QSAR, molecular docking and molecular dynamics simulation, *J Asian Nat Prod Res* 27 (2025) 442–459, <https://doi.org/10.1080/10286020.2024.2402369>.
- [9] M. Pei, A. Qian, L. Cao, Z. Wang, Y. Lu, C. Yan, T. Liang, *In silico* design of novel potential isonicotinamide-based glycogen synthase kinase-3 $\beta$  (GSK-3 $\beta$ ) inhibitors: 3D-QSAR, molecular docking, molecular dynamics simulation and ADMET studies, *New J Chem* 10 (2025) 1039, <https://doi.org/10.1039/D4NJ01951B>. D4NJ01951B.
- [10] D. Panigrahi, S.K. Sahu, Computational approaches: atom-based 3D-QSAR, molecular docking, ADME-Tox, MD simulation and DFT to find novel multi-targeted anti-tubercular agents, *BMC Chem* 19 (2025) 39, <https://doi.org/10.1186/s13065-024-01357-2>.
- [11] B. Saroha, G. Kumar, R. Kumar, M. Kumari, S. Kumar, A minireview of 1,2,3-triazole hybrids with O-heterocycles as leads in medicinal chemistry, *Chem Biol Drug Des* 100 (2022) 843–869, <https://doi.org/10.1111/cbdd.13966>.
- [12] L.M.R. Orlando, L.D.S. Lara, G.C. Lechuga, G.C. Rodrigues, O.G. Pandoli, D.S. De Sá, M.C.D.S. Pereira, Anti-trypanosomal activity of 1,2,3-triazole-based hybrids evaluated using in vitro preclinical translational models, *Biology* 12 (2023) 1222, <https://doi.org/10.3390/biology12091222>.
- [13] B. Zhang, Comprehensive review on the anti-bacterial activity of 1,2,3-triazole hybrids, *Eur J Med Chem* 168 (2019) 357–372, <https://doi.org/10.1016/j.ejmech.2019.02.055>.
- [14] B. Aneja, M. Azam, S. Alam, A. Perwez, R. Maguire, U. Yadava, K. Kavanagh, C.G. Daniliuc, M.M.A. Rizvi, Q. Mohd. R. Haq, M. Abid, Natural product-based 1,2,3-triazole/sulfonate analogues as potential chemotherapeutic agents for bacterial infections, *ACS Omega* 3 (2018) 6912–6930, <https://doi.org/10.1021/acsomega.8b00582>.
- [15] D. Shivakumar, J. Williams, Y. Wu, W. Damm, J. Shelley, W. Sherman, Prediction of absolute solvation free energies using molecular dynamics free energy perturbation and the OPLS force field, *J Chem Theor Comput* 6 (2010) 1509–1519, <https://doi.org/10.1021/ct900587b>.
- [16] S. Zhang, A. Golbraikh, S. Oloff, H. Kohn, A. Tropsha, A novel automated lazy learning QSAR (ALL-QSAR) approach: method development, applications, and virtual screening of chemical databases using validated ALL-QSAR models, *J Chem Inf Model* 46 (2006) 1984–1995, <https://doi.org/10.1021/ci060132x>.
- [17] A. Golbraikh, A. Tropsha, QSAR modeling using chirality descriptors derived from molecular topology, *J Chem Inf Comput Sci* 43 (2003) 144–154, <https://doi.org/10.1021/ci025516b>.
- [18] G. Verma, M.F. Khan, W. Akhtar, M.M. Alam, M. Akhter, O. Alam, S.M. Hasan, M. Shaquiquzzaman, Pharmacophore modeling, 3D-QSAR, docking and ADME prediction of quinazoline based EGFR inhibitors, *Arab J Chem* 12 (2019) 4815–4839, <https://doi.org/10.1016/j.arabjc.2016.09.019>.
- [19] E. Gordon, N. Mouz, E. Duée, O. Dideberg, The crystal structure of the penicillin-binding protein 2x from *Streptococcus pneumoniae* and its acyl-enzyme form: implication in drug resistance 1 1 Edited by R. Huber, *J Mol Biol* 299 (2000) 477–485, <https://doi.org/10.1006/jmbi.2000.3740>.
- [20] Y. Liu, X. Yang, J. Gan, S. Chen, Z.-X. Xiao, Y. Cao, CB-Dock2: improved protein–ligand blind docking by integrating cavity detection, docking and homologous template fitting, *Nucleic Acids Res* 50 (2022) W159–W164, <https://doi.org/10.1093/nar/gkac394>.
- [21] S.M. Bufarwa, M. Belaidi, L.M. Abbass, D.K. Thbayh, Anti-cancer Activity, DFT, Molecular Docking, ADMET, and molecular dynamics simulations investigations of schiff base derived from 2,3-diaminophenazine and its metal complexes, *Appl Organomet Chem* 39 (2025) e7953, <https://doi.org/10.1002/aoc.7953>.
- [22] F. Neese, Software update: the ORCA program system, version 5.0, *WIREs Comput Molec Sci* 12 (2022) e1606, <https://doi.org/10.1002/wcms.1606>.
- [23] J. Tixier, G. Dusserre, S. Rault-Doumax, J. Ollivier, C. Bourelly, OSIRIS: software for the consequence evaluation of transportation of dangerous goods accidents, *Environ Model Software* 17 (2002) 627–637, [https://doi.org/10.1016/S1364-8152\(02\)00025-7](https://doi.org/10.1016/S1364-8152(02)00025-7).
- [24] A. Daina, O. Michielin, V. Zoete, SwissADME: a free web tool to evaluate pharmacokinetics, drug-likeness and medicinal chemistry friendliness of small molecules, *Sci Rep* 7 (2017) 42717, <https://doi.org/10.1038/srep42717>.
- [25] S.M. Bufarwa, R.M. El-Sefait, D.K. Thbayh, M. Belaidi, R.K. Al-Shemary, Rema.M. Abdusamea, M.M. El-Ajaily, B. Fiser, H.A. Bader, A.A. Saleh, M.M. Bufarwa, Antituberculosis, antimicrobial, antioxidant, cytotoxicity and anti-inflammatory activity of Schiff base derived from 2,3-diaminophenazine moiety and its metal(II) complexes: structural elucidation, computational aspects, and biological evaluation, *Rev Inorg Chem* 45 (2025) 105–124, <https://doi.org/10.1515/revic-2024-0007>.